Discover Oncology

Analysis

Establishment of a m6 A-associated lncRNAs-derived risk model for enhanced patient prognosis stratification and personalized therapy approaches in bladder cancer

Renhu Chen[1] · **Yuqing Ye**[2] · **Yuxuan Zheng**[3]

Received: 8 February 2025 / Accepted: 9 May 2025
Published online: 22 May 2025
© The Author(s) 2025 OPEN

Abstract

Introduction Bladder cancer (BCa) is a leading malignancy in the urinary tract system, often resulting in poor prognosis due to rapid relapse and metastasis, with a low 5-year survival rate. Although the role of N6-methyladenosine (m6A) methylation and long noncoding RNAs (lncRNAs) is implicated in BCa progression, research on how lncRNAs influence BCa prognosis and potential therapeutic interventions remains scarce.

Methods RNA expression profiles and gene mutations for 406 BCa patients were retrieved from the The Cancer Genome Atlas (TCGA) database. A comprehensive dataset was established to correlate lncRNAs with 21 identified m6A-associated genes, categorized into writers, erasers, and readers. Pearson correlation analysis between these m6A genes and lncRNAs was performed and a prognostic model derived from m6A-associated lncRNAs was developed. Immune infiltration was analyzed using multiple evaluative methods and the correlation between single nucleotide variant (SNV) mutations and drug sensitivity was assessed for the correlative relationship with the m6A-associated lncRNA-derived risk scores.

Results We identified 3,462 m6A-associated lncRNAslinked to BCa prognosis, of which 238 lncRNAs showed significant associations with overall survival in BCa patients. A m6A-associated lncRNA-derived risk model comprising 26 selected lncRNAs was developed using Least Absolute Shrinkage and Selection Operator (LASSO) Cox regression, where BCa patients with higher m6A-associated lncRNA-derived risk scores had poorer outcomes. The prognostic significance and reliability was validated, with an area under the curve (AUC) value exceeding 0.7 at multiple time points. Additionally, a nomogram integrating clinical features and m6A-associated lncRNA-derived risk scores had enhanced prognostic accuracy over other clinical indicators, with promise for clinical decision-making. A negative correlation was observed between m6A-associated lncRNA-derived risk scores and tumor mutational burden (TMB). Moreover, patients with high m6A-associated lncRNA-derived risk score group showed significant enrichment of regulatory T cells (Tregs), M2 macrophages, and fibroblasts, highlighting the potential involvement of immune and stromal cells in these BCa patients.

Conclusion These findings highlight the prognostic value and clinical relevance of m6A-associated lncRNAs in BCa for future patient stratification and personalized therapy approaches.

Keywords Bladder cancer · Long non-coding RNAs · Prognosis · Immune · Mutation · M6 A methylation

✉ Yuxuan Zheng, zhyx195@163.com | [1]Department of Sexual Medcine and Andrology, The Fifth People's Hospital of Shunde (Longjiang Hospital of Shunde District), Foshan, China. [2]School of Medicine, Dentistry and Nursing, University of Glasgow, Glasgow, UK. [3]Department of Urology, The Fourth Affiliated Hospital of China Medical University, Shenyang 110032, China.

1 Introduction

Bladder cancer (BCa) is one of the most prevalent malignancies in the urinary tract system, with invasive tumors often associated with poor prognosis [1, 2]. Despite advancements in diagnosis, the 5-year survival rate for BCa remains low [1], which is largely attributed to rapid relapse and distant metastasis[2]. Hence, it is essential to comprehend the molecular aspects of BCa progression to improve these outcomes. The development of BCa involves a complex interplay of genetic and epigenetic alterations [3–5]. Many distinct RNA modifications in this context have been identified, highlighting m6 A methylation as one of the most prevalent ones [6]. For example, research by Cheng and colleagues demonstrated significantly elevated m6 A levels in BCa tumor tissues, and identified that methyltransferase-like 3 (METTL3), a key enzyme in the m6 A "writer" complex, facilitates BCa progression by modulating the AFF4/MYC signaling pathway through m6 A modifications [7].

Long noncoding RNAs (lncRNAs) [8], which are over 200 nucleotides long, typically do not have protein-coding functions [9]. Further, lncRNAs show unique tissue-specific gene expression patterns [10, 11], which are closely involved in BCa incidence and function primarily by interacting with gene-regulatory proteins and microRNAs [12]. For instance, the rs62483508 G > A variant was identified in the lncRNA BCCE4 as being associated with a decreased risk of BCa. The protective A allele disrupts miR-328-3p binding, preventing USP18 degradation and attenuating programmed death-ligand 1 (PD-L1)/programmed death-1 (PD-1) interactions, influencing immune response regulation in tumorigenesis [13]. Research on the role of lncRNAs in stratification of patient prognosis in BCa remains limited [11], indicating the need for further analysis.

In this study, we identified a profile of m6 A-associated [14] lncRNAs associated with BCa prognosis; of 3,462 lncRNAs studied, 238 were significantly linked to the overall survival (OS) in BCa patients. A m6 A-associated lncRNAs-derived risk model using LASSO Cox regression was developed, and the validation showed strong predictive reliability (AUC > 0.7). Furthermore, a nomogram combining clinical features and the m6 A-associated lncRNA risk score improved prognostic accuracy, outperforming traditional clinical indicators. Notably, BCa patients with higher m6 A-associated lncRNAs-derived risk scores showed significant enrichment of regulatory T cells, M2 macrophages, and fibroblasts. These findings underscore the prognostic value and clinical significance of m6 A-associated lncRNAs in BCa, offering valuable insights into patient stratification and personalized treatment strategies.

2 Methods

2.1 Acquisition of transcriptomic data

RNA expression profiles and corresponding clinical data for BCa (n = 406) were retrieved from the TCGA database. Additionally, RNAseq data from The Cancer Genome Atlas Urothelial Bladder Carcinoma (TCGA-BLCA) were combined to create a dataset for correlating lncRNAs with m6 A-associated genes.

2.2 Acquisition of N6-methyladenosine genes

A total of 21 m6 A regulators were identified, including 8 writers (METTL3, METTL14, RBM15, RBM15B, WTAP, KIAA1429, CBLL1, ZC3H13), 2 erasers (ALKBH5, FTO), and 11 readers (YTHDC1, YTHDC2, YTHDF1, YTHDF2, YTHDF3, IGF2BP1, HNRNPA2B1, HNRNPC, FMR1, LRPPRC, ELAVL1).

2.3 Correlation analysis

The Pearson algorithm rcorr function from the Hmisc package was employed for analysis and a correlation heatmap was generated using the pheatmap package for visualization.

2.4 Establishing risk features associated with N6-methyladenosine-associated lncRNAs

Initially, univariate Cox analysis was conducted to extract m6 A-associated lncRNAs with prognostic significance. Least Absolute Shrinkage and Selection Operator (Lasso) regression was then applied to further screen these prognostic genes to develop a prognostic model. The predictive variations among BCa patients with different m6 A-associated lncRNAs-derived risk scores were then examined.

2.5 Assessment of the independence and validity of the N6-methyladenosine-associated lncRNAs-derived model

A nomogram including age, m6 A-associated lncRNA-derived risk score, and pathological stage as independent prognostic factors was developed. Furthermore, Kaplan–Meier survival curves were drawn, and log-rank tests were performed to evaluate statistical significance. Calibration was conducted to assess the accuracy of the nomogram. Decision curve analysis (DCA) was employed to further evaluate the overall benefit of the nomogram in comparison to clinical features.

2.6 Correlation analysis of the prognostic model with tumor immunity

The level of immune infiltration in patients with BCa from the TCGA database was determined using the IOBR software, which incorporated results from seven evaluative methods. Subsequently, gene set variation analysis (GSVA) was conducted using the R package with immune-associated characteristics for single sample gene set enrichment analysis (ssGSEA) analysis on the genes within the prognostic risk assessment model.

2.7 SNV mutations and drug sensitivity

The "maftools" software was utilized to retrieve the gene mutation landscape for BCa patients from the TCGA database. Detailed gene mutation files were merged with m6 A-associated lncRNAs-derived risk scores. Additionally, the R package "oncoPredict" was employed to calculate the half-maximal inhibitory concentration (IC50) of common chemotherapy drugs to assess the potential correlative relationship analysis. Wilcoxon rank-sum tests were conducted to compare IC50 values between the BCa patients of different m6 A-associated lncRNA-derived risk groups.

3 Results

3.1 Identification of N6-methyladenosine-associated lncRNAs in bladder cancer patients

Principal Component Analysis (PCA) analysis of the TCGA dataset suggested several differences between the distribution in the training and testing sets (Fig. 1A). The m6 A-lncRNA co-expression network identified 3,462 m6 A-associated lncRNAs, visualized using a Sankey diagram, shown in Fig. 1B, which were further filtered for those with prognostic significance. Of these, 238 m6 A-associated lncRNAs were found to have a significant association with the OS of BCa patients (Fig. 1C). The correlations between m6 A genes and m6 A-associated lncRNAs identified with prognostic significance in the combined dataset are depicted in Fig. 1D. Among these RP11-81,519.4 had a positive correlation with both m6 A eraser and reader expression, while RP3-508I15.21 displayed a high negative correlation with several m6 A erasers and readers, suggesting RP3-508I15.21 and RP11-81519.4 might be crucial regulators of m6 A modification in BCa.

3.2 Construction of the N6-methyladenosine-associated lncRNA risk model

The prognostic model was developed using LASSO Cox regression analysis (Fig. 2A, B). Under optimal regularization parameters, the final selection included 26 lncRNAs (RASAL2-AS1, ARHGAP22-IT1, TSTD3, EAF1-AS1, RP11-3 J1.1, OSBPL10-AS1, RP11-259 K5.2, RP11-815I9.4, RNF217-AS1, RP11-228B15.4, THUMPD3-AS1, RP11-881M11.4, CTD-2231H16.1, RP11-689P11.2, RP11-199 F11.2, OCIAD1-AS1, RP11-428 J1.5, IGF2BP2-AS1, AC010731.2, FOXC2-AS1, RP11-366L5.1, ARHGAP5-AS1, CTD-2240E14.4, RP3-508I15.21, RP11-385D13.3, RP11-446H18.5). Further, 18 of the 26 lncRNAs were identified as risk factors, while 8 were protective factors (Fig. 2C), with the highest risk score seen for ARHGAP22-IT1. The distribution of risk

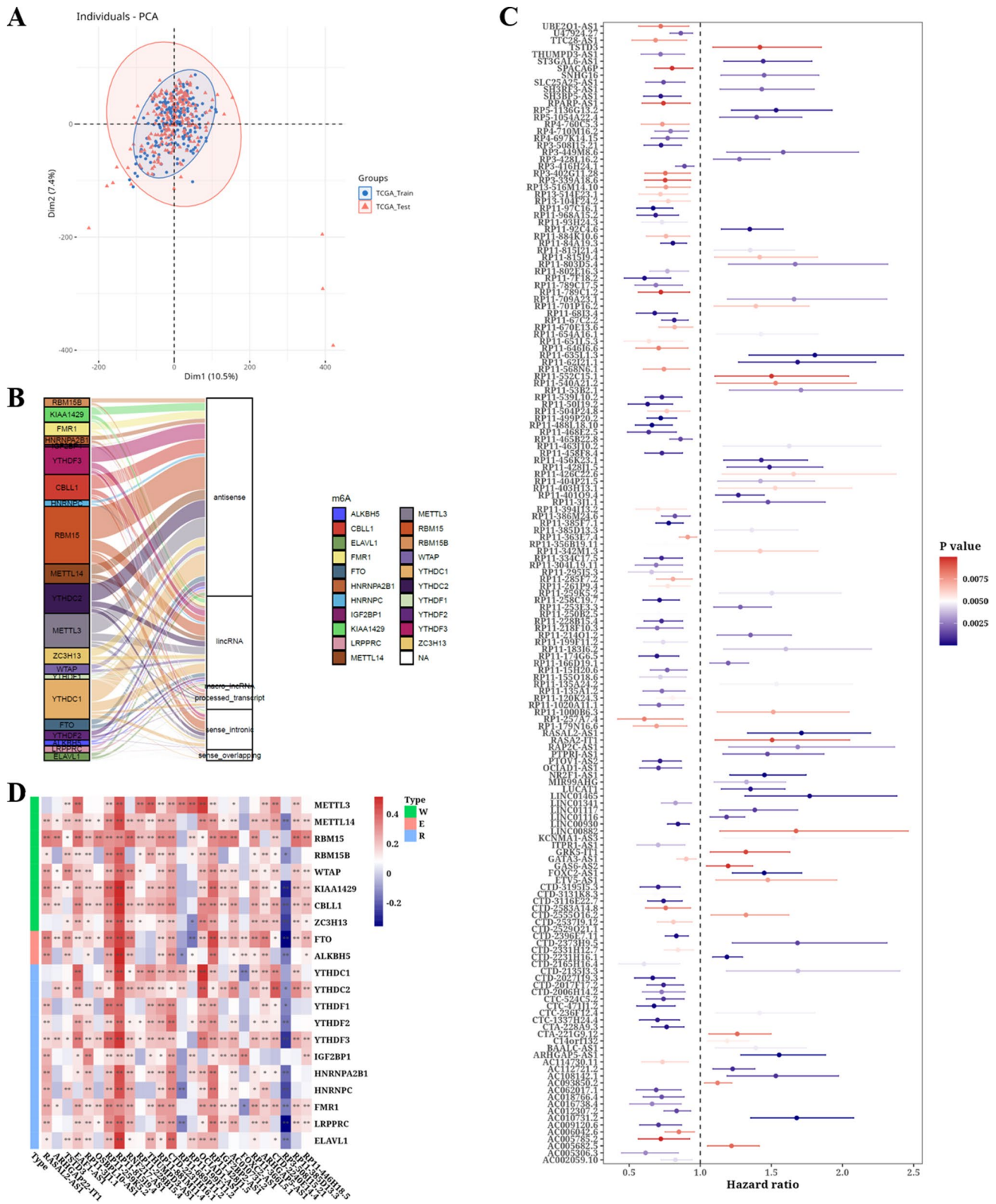

Fig. 1 Identification of N6-methyladenosine (m6 A)-associated lncRNAs in Bladder Cancer (BCa) Patients. **A** Principal Component Analysis (PCA) analysis of training and testing sets of bladder cancer (BCa)patients in The Cancer Genome Atlas (TCGA) dataset. **B** Sankey diagram illustrating the association between m6a regulators and lncRNAs.. The criteria for selection of m6 A-associated lncRNAs: significantly associated with at least one of the 21 m6 A genes, with |Pearson R|> 0.3 and $p < 0.001$, derived on the expression data for 21 m6 A genes and lncRNAs from the TCGA dataset. **C** Illustration of the 238 m6 A-associated lncRNAs significantly associated with the overall survival (OS) of bladder cancer (BCa) patients and corresponding hazard ratio value. **D** The heatmap illustrating the correlations between m6 A genes and m6 A-associated lncRNAs identified with prognostic significance in the combined dataset

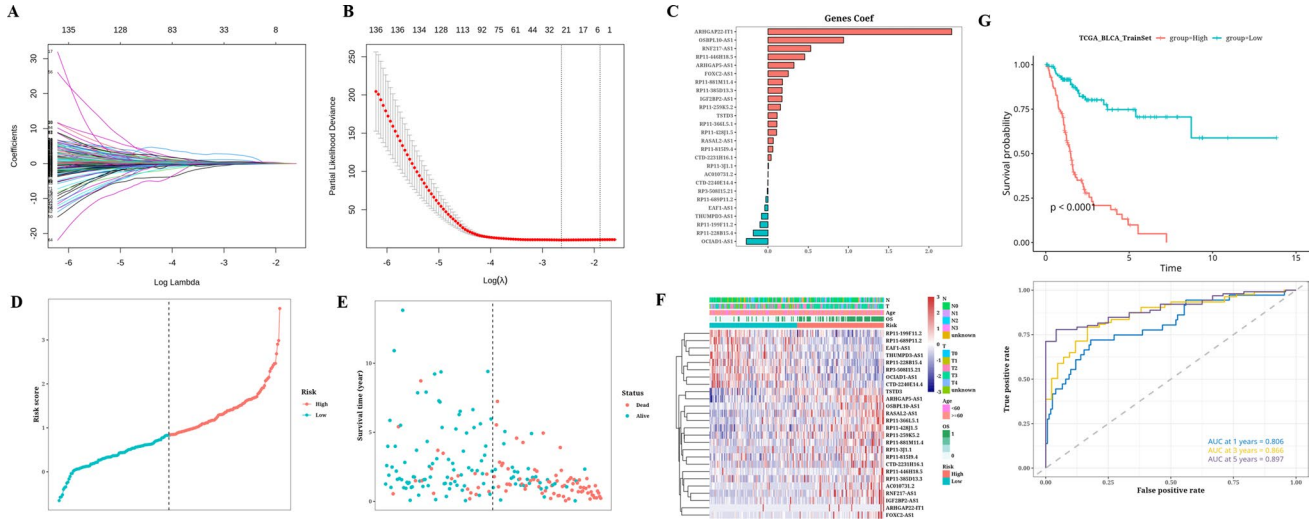

Fig. 2 Construction of the N6-methyladenosine (m6 A)-associated lncRNA-derived Risk Model. **A**, **B** Least Absolute Shrinkage and Selection Operator (LASSO) Cox regression analysis was employed to further screen the lncRNAs with prognostic significance. **C**. Bar plot illustrating the coefficients of each hub lncRNA in the m6 A-associated lncRNA-derived risk model. **D** The distribution of m6 A-associated lncRNA-derived risk score of each bladder cancer (BCa) patient in the training set. **E** The scatter dot plot illustrates the survival time and status of bladder cancer (BCa) patients with different lncRNA-derived risk scores in the training set. **F** The heatmap plot shows detailed clinical factors, including age, pathological N stage, and pathological T stage, of bladder cancer (BCa) patients with different lncRNA-derived risk scores in the training set. **G** The survival analysis using the KM curve of bladder cancer (BCa) patients in different lncRNA-derived risk groups in the TCGA-BLCA cohort and ROC analysis highlighting area under the curve (AUC) values greater than 0.8 at 1, 3, and 5 years

levels between BCa patients with different m6 A-associated lncRNA-derived risk scores is illustrated in Fig. 2D, while the patient survival status and duration are shown in Fig. 2E. The relative expression levels of the 26 model lncRNAs for each patient are presented in Fig. 2F. Survival analysis indicated that BCa patients with high m6 A-associated lncRNA-derived risk scores exhibited poorer prognosis ($p < 0.05$), with AUC values exceeding 0.8 at examined time points (Fig. 2G). These results suggest that the prognosis stratification efficacy of the m6 A-associated lncRNA-derived risk model was optimalof.

3.3 Validation of the m6 A-associated lncRNA-derived risk model

We calculated the lncRNA-derived risk score for each patient in the testing set (Fig. 3A–C), the entire dataset (Fig. 3E–G), and the clinical characteristic profiles. Survival curves and ROC curves for the testing set and the entire dataset are shown in Fig. 3D and H, respectively. We found that the BCa patients with higher m6 A-associated lncRNA-derived risk scores exhibited poorer prognosis ($p < 0.05$), with AUC values exceeding 0.7 at different indicated time points in the entire set.

3.4 Analysis of the N6-methyladenosine-associated lncRNA-derived nomogram

A nomogram was created using clinical information and m6 A-associated lncRNA-derived risk scores to quantify the OS of BCa patients more accurately (Fig. 4A), to guide future treatment decisions. C index analyses indicated better performance of the nomogram than other clinical indicators, demonstrating its effectiveness in predicting patient prognosis and use as a clinical decision-making tool (Fig. 4B, C). Prognostic Receiver Operating Characteristic (ROC) analysis was conducted to thoroughly evaluate the accuracy of the nomogram, which yielded AUC values of 0.715, 0.774, and 0.787 at the indicated time points (Fig. 4D–F), which proved to be superior to m6 A-associated lncRNA-derived risk model at 3 years and 5 years.

3.5 Clinical pathological analysis of the N6-methyladenosine-associated lncRNA-derived bladder cancer risk model

We analyzed the differences in OS between patients with BCa from m6 A-associated lncRNA-derived risk groups stratified by clinical pathological characteristics within the TCGA cohort. The BCa patients in the lower m6 A-associated lncRNA-derived risk group consistently exhibited superior OS across subgroups of age under and over 60, N0 and N1 stages, T2

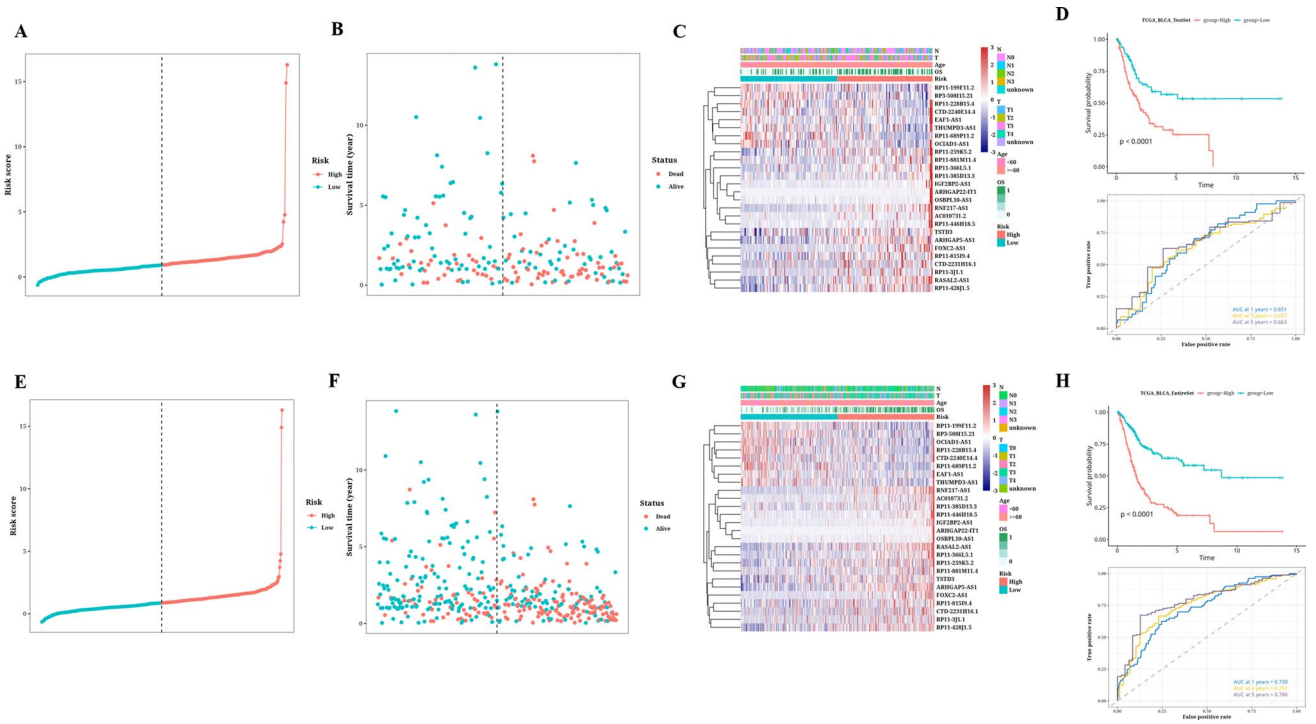

Fig. 3 Validation of the N6-methyladenosine (m6 A)-associated lncRNA-derived risk model. **A**, **B** The scatter dot plot shows the distribution of m6 A-associated lncRNA-derived risk score of each bladder cancer (BCa) patient in the testing set (**A**) and the survival time and status of bladder cancer (BCa) patients with different lncRNA-derived risk scores (**B**). **C** The heatmap shows detailed clinical factors, including age, pathological N stage, and pathological T stage, of bladder cancer (BCa) patients with different lncRNA-derived risk scores in the testing set. **D** The survival analysis using the Kaplan–Meier (KM) curve of bladder cancer (BCa) patients in different lncRNA-derived risk groups in the testing cohort and ROC analysis highlighting area under the curve (AUC) values greater than 0.65 at 1, 3, and 5 years. **E**, **F** The scatter dot plot shows the distribution of m6 A-associated lncRNA-derived risk score of each bladder cancer (BCa) patient in the entire set (**E**) and the survival time and status of BCa patients with different lncRNA-derived risk scores (**F**). **G** The heatmap shows detailed clinical factors, including age, pathological N stage, and pathological T stage, of bladder cancer (BCa) patients with different lncRNA-derived risk scores in the entire set. **H** The survival analysis using the Kaplan–Meier (KM) curve of the bladder cancer (BCa) patient in different lncRNA-derived risk groups in the entire cohort and Receiver Operating Characteristic (ROC) analysis highlighting area under the curve (AUC) values greater than 0.7 at 1, 3, and 5 years.

and advanced stages (Fig. 5A–F). Chi-square tests utilized to analyze the compositional differences in age, pathological N stage, and pathological T stage between BCa patients of different m6 A-associated lncRNA-derived risk groups revealed a significant difference in the composition of pathological T stage ($p < 0.05$) (Fig. 5G–I).

3.6 Further validation of grouping ability of the N6-methyladenosine-associated lncRNA-derived model

PCA was performed to assess the differences in gene expression profiles between patients with BCa of different m6 A-associated lncRNA-derived risk groups for gross gene expression (A), the 3,462 m6 A-associated lncRNAs (B), 21 m6 A genes (C), and the 26 modeled m6 A-associated lncRNAs (D). Figure 6A, B illustrate the prominently distinct distribution of BCa patients with different m6 A-associated lncRNA-derived risk score groups. These findings indicate that the m6 A-associated lncRNA-derived risk model can effectively differentiate the gross gene expression and lncRNA expression profile of BCa patients.

3.7 Mutation analysis of bladder cancer patients of different N6-methyladenosine-associated lncRNA-derived risk groups

An overview of mutations in BCa patients is depicted in Fig. 7A, with missense mutations identified as the most common type of mutation and the top three frequently mutated genes were TTN, TP53, and MUC16. We also examined representative gene variants in BCa patients of different m6 A-associated lncRNA-derived risk groups (Fig. 7B, C). The top five genes with the highest mutation frequency were TP53, TTN, KMT2D, ARID1 A, and MUC16 in the BCa

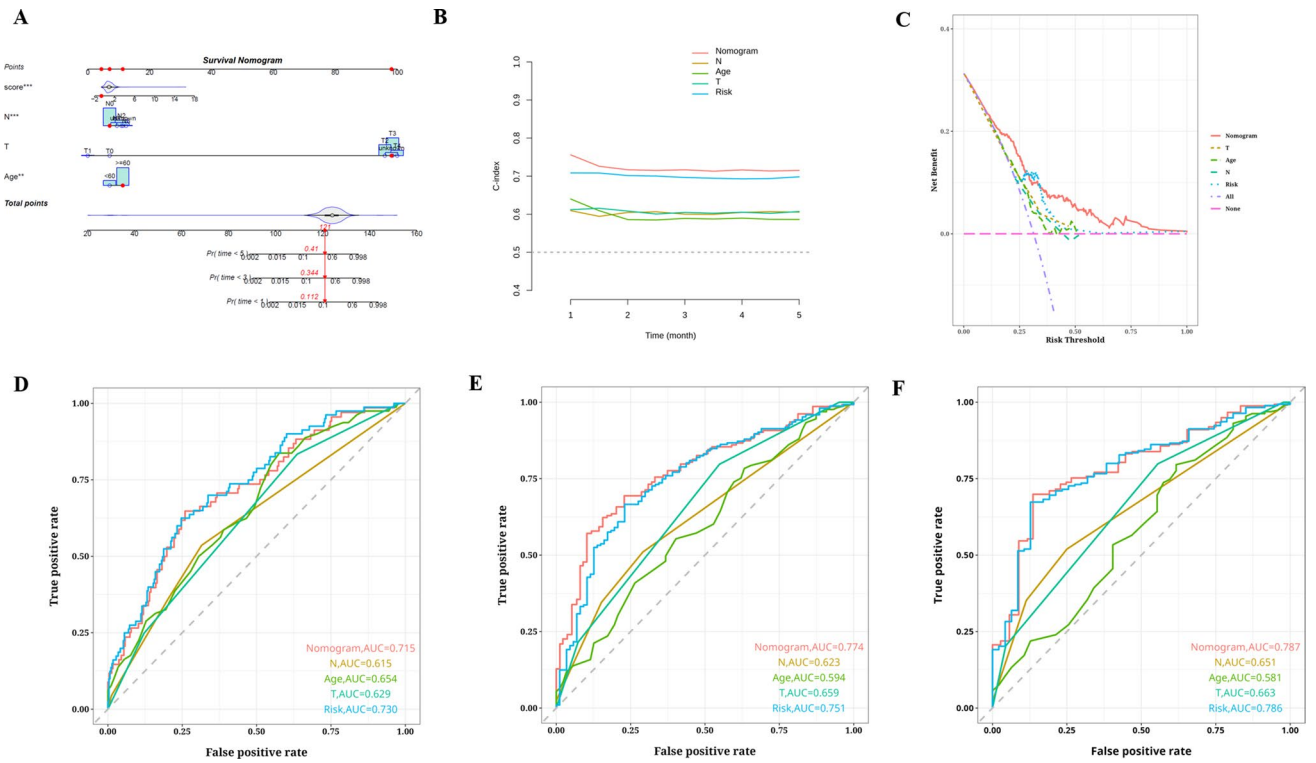

Fig. 4 Construction of the N6-methyladenosine (m6 A)-associated lncRNA-derived Nomogram. **A** The m6 A-associated lncRNA-derived nomogram was constructed by also integrating various clinical characteristics. **B** The C-index analysis of the constructed m6 A-associated lncRNA-derived nomogram. **C** The Decision curve analysis (DCA) analysis of the constructed m6 A-associated lncRNA-derived nomogram. **D**–**F** Prognostic Receiver Operating Characteristic (ROC) analysis of the constructed m6 A-associated lncRNA-derived nomogram, along with calculated area under the curve (AUC) values of different modeled factors at different time points: 1 (**D**), 3 (**E**), and 5 (**F**) years

patients of higher m6 A-associated lncRNA-derived risk score, while the top five genes with the highest mutation frequency in the BCa patients of lower m6 A-associated lncRNA-derived risk score were TP53, TTN, KDM6 A, MUC16, and ARID1 A. We also investigated the mutation co-occurrence among the top 25 genes and identified significant co-occurrence of mutations between TP53 and multiple genes, including TTN and KDM6 A (Fig. 7D). Calculated TMB values for BCa patients within different m6 A-associated lncRNA-derived risk groups revealed no significant differences (Fig. 7E). Furthermore, a correlation analysis between m6 A-associated lncRNA-derived risk scores and TMB showed a negative correlation ($R = -0.12$, $p = 0.021$) (Fig. 7F). Additionally, we explored the prognostic impact of TMB grouping combined with the m6 A-associated lncRNA-derived risk grouping on OS. The survival analysis suggested that BCa patients with lower TMB levels and higher m6 A-associated lncRNA-derived risk scores were associated with poorer prognosis (Fig. 7G), further validating the negative correlation between m6 A-associated lncRNA-derived risk scores and TMB levels.

3.8 Immune characterization and drug sensitivity analysis of N6-methyladenosine-associated lncRNA-derived risk groups

We utilized seven methods, including CIBERSORT, to determine the level of immune and immune regulatory cell infiltration in each BCa sample of the TCGA-BLCA cohort (Fig. 8A). We foond that Tregs, M2 macrophages, and fibroblasts were highly enriched in the BCa samples with higher m6 A-associated lncRNA-derived risk scores. We further examined the differences in drug resistance between BCa patients with different TMB m6 A-associated lncRNA-derived risk groups. We identified Docetaxel_1007, Staurosporine_1034, Luminespib_1559, and Docetaxel_1819 as potential candidate drugs to treat BCa patients with higher m6 A-associated lncRNA-derived risk scores (Figs. 8B–E). These initial results might potentially assist in selecting the most optimal drugs for the clinical treatment of BCa.

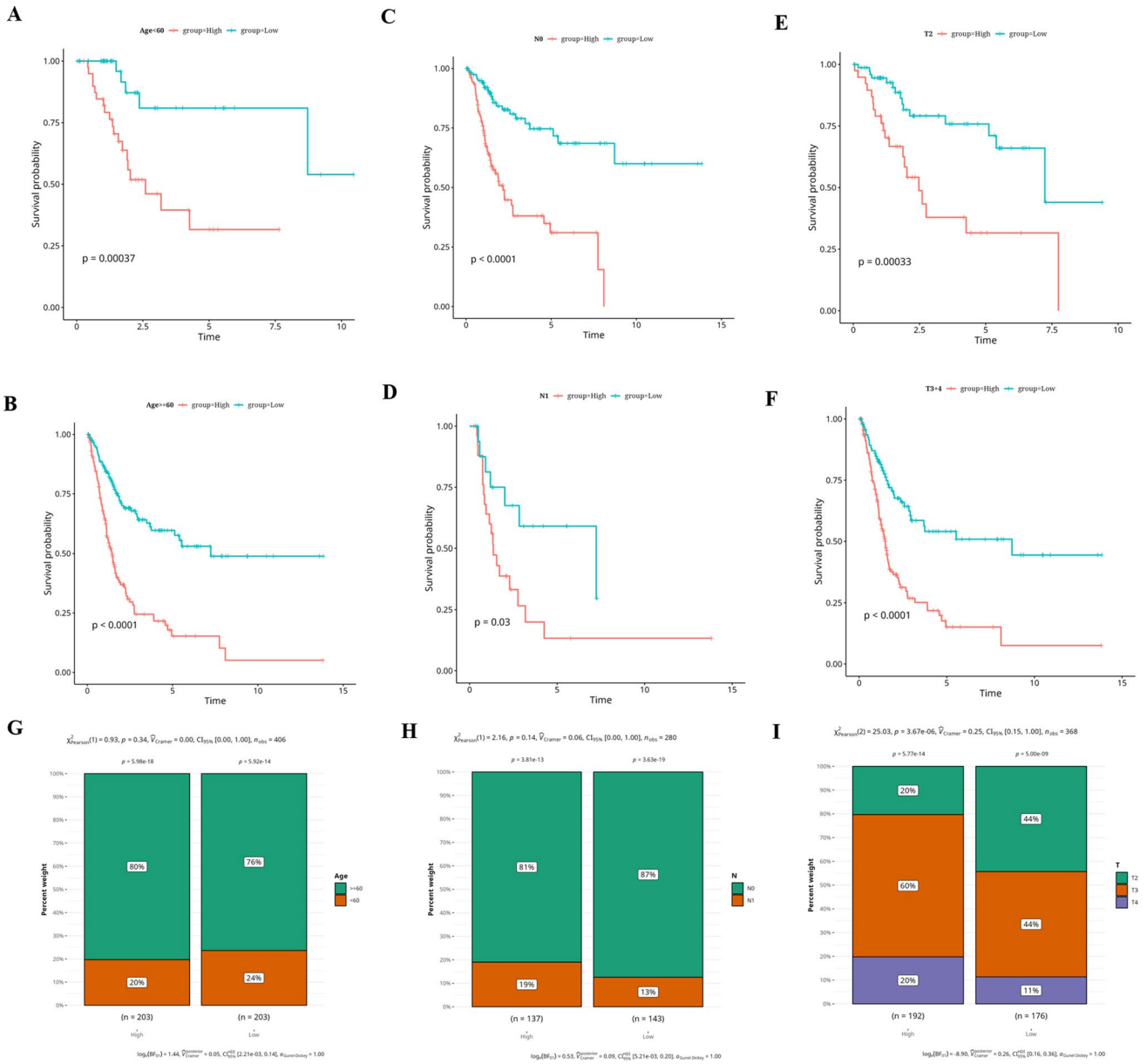

Fig. 5 Clinical pathological analysis of bladder cancer (BCa) prognostic features of the N6-methyladenosine (m6 A)-associated lncRNA-derived Risk Model. **A** The survival analysis using the Kaplan–Meier (KM) curve of bladder cancer (BCa) patients in different lncRNA-derived risk groups with age under 60. **B** The survival analysis using the Kaplan–Meier (KM) curve of bladder cancer (BCa) patients in different lncRNA-derived risk groups with age over 60. **C** The survival analysis using the Kaplan–Meier (KM) curve of bladder cancer (BCa) patients of N0 in different lncRNA-derived risk groups. **D** The survival analysis using the Kaplan–Meier (KM) curve of the bladder cancer (BCa) patients of N1 in different lncRNA-derived risk groups. **E** The survival analysis using the Kaplan–Meier (KM) curve of bladder cancer (BCa) patients of T2 in different lncRNA-derived risk groups. **F** The survival analysis using the Kaplan–Meier (KM) curve of the bladder cancer (BCa) patients of T3 + 4 in different lncRNA-derived risk groups

4 Discussion

This report is a comprehensive analysis conducted to identify m6 A-associated lncRNAs associated with BCa prognosis [11, 15–17]. We identified 3462 m6 A-associated lncRNAs, with 238 demonstrating significant associations with OS in BCa patients. A m6 A-associated lncRNA-derived risk model using 26 selected lncRNAs was developed using LASSO Cox regression analysis, with BCa patients with higher m6 A-associated lncRNA-derived risk score exhibiting poorer outcomes The prognostic significance of the model was validated, with AUC values over 0.7 across multiple time

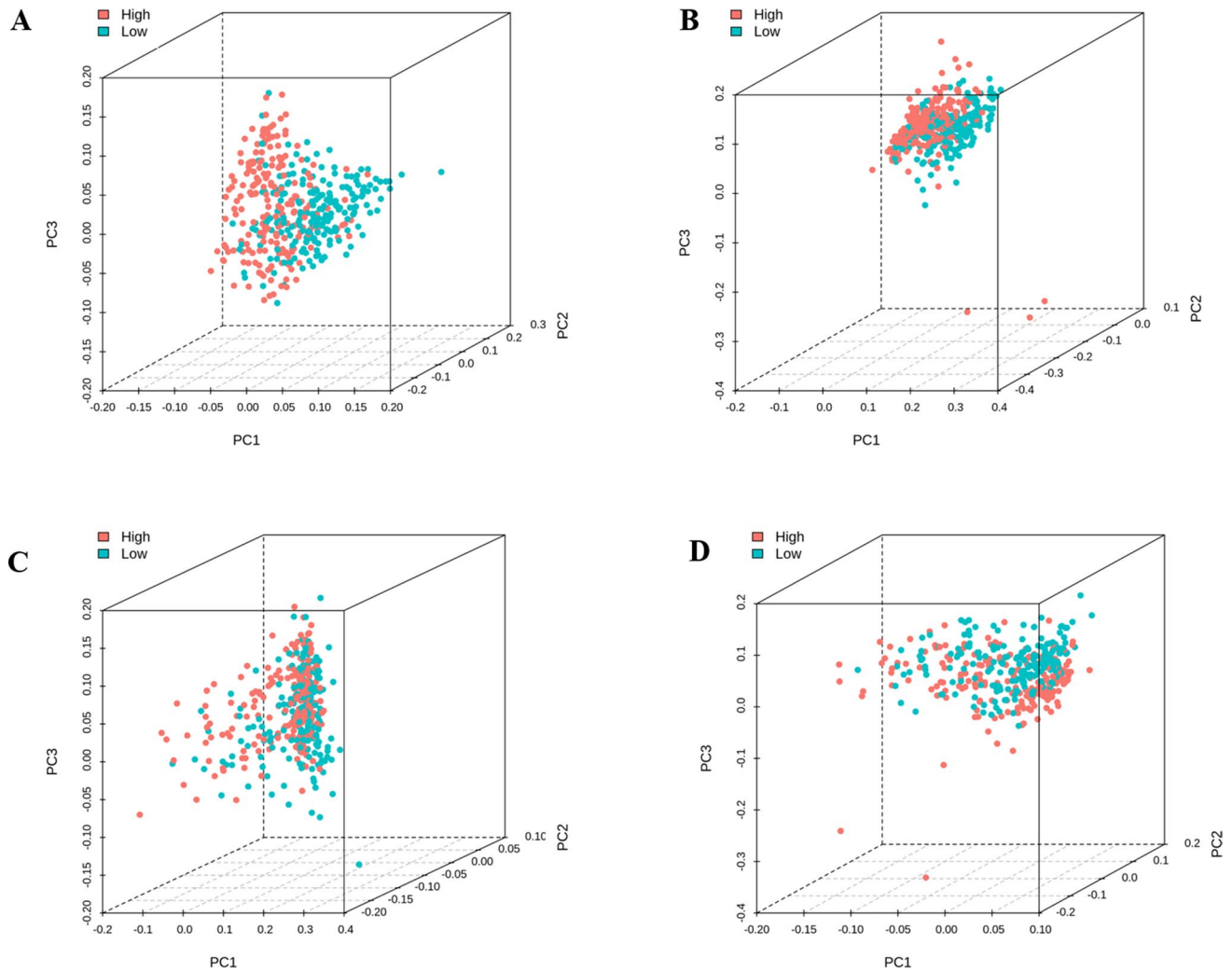

Fig. 6 Further validation of stratification ability of the N6-methyladenosine (m6 A)-associated lncRNA-derived Model. **A** PCA analysis detecting the stratification of the overall survival (OS) patients of different m6 A-associated lncRNA-derived risk scores based on gene expression profile. **B** PCA analysis detecting the stratification of OS patients of different m6 A-associated lncRNA-derived risk scores based on 3,462 m6 A-associated lncRNAs. **C** PCA analysis detecting the stratification of OS patients of different m6 A-associated lncRNA-derived risk scores based on 21 m6 A genes. **D** PCA analysis detecting the stratification of OS patients of different m6 A-associated lncRNA-derived risk scores based on the 26 m6 A-associated lncRNA expression profile

points, supporting its reliability in predicting BCa patient outcomes. A nomogram including clinical features and risk scores showed improved prognostic accuracy, outperforming other clinical indicators and demonstrating its utility as a clinical decision-making tool. A notable negative correlation between m6 A-associated lncRNA-derived risk scores and TMB was observed. Intriguingly, Tregs, M2 macrophages, and fibroblasts were highly enriched in the BCa samples in the high m6 A-associated lncRNA-derived risk group.

Although their molecular mechanisms are not fully understood, lncRNAs become well-acknowledged as key regulators in BCa development. For instance, lncRNA RP11-89 was shown to promote BCa tumorigenesis through the manipulation of the miR-129-5p/PROM2 axis [18]. The role of lncRNAs was shown to be vitally implicated in lymphatic metastasis, which is a major pathway in BCa. Additionally, lncRNA BLACAT3 was involved in promoting angiogenesis and hematogenous metastasis by activating NF-κB signaling through m6 A-mediated RNA stabilization and recruitment of YBX3 [19]. Another lncRNA ELNAT1 found in extracellular vesicles (EVs) secreted by BCa cells was shown to interact with endothelial cells to promote lymphangiogenesis through SUMOylation. LncRNA ELNAT1 induced UBC9 overexpression, leading to the SUMOylation of hnRNPA1, which facilitated inclusion in EVs via the ESCRT complex [20]. These findings suggested lncRNAs were intricately associated with lymphatic metastasis in BCa, making lncRNAs as potential therapeutic targets for LN metastatic BCa.

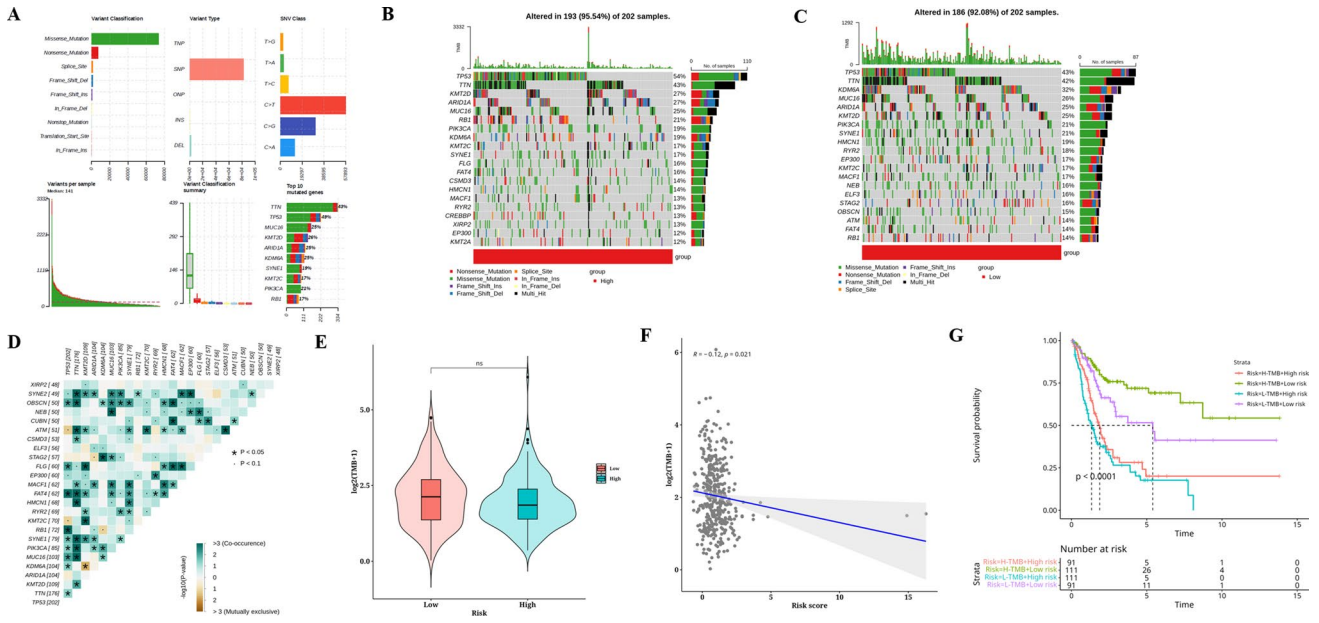

Fig. 7 Single Nucleotide Variant (SNV) Mutation Analysis of Bladder Cancer (BCa) Patients of Different N6-methyladenosine (m6 A)-associated lncRNA-derived Risk Groups. **A** The overview of the mutation status in bladder cancer (BCa) patients, including mutation type, mutation frequency, mutation classification summarization, and SNV class. **B** The waterfall plot illustrating mutation type and mutation frequency in the bladder cancer (BCa) patients of relatively higher m6 A-associated lncRNA-derived risk scores. **C** The waterfall plot illustrating mutation type and mutation frequency in the bladder cancer (BCa) patients in the low m6 A-associated lncRNA-derived risk score group. **D** The mutation co-occurrence analysis among the top 25 genes (the *p*-value for co-concurring is reflected by the depth of color). **E** The violin plot showing the tumor mutational burden (TMB) values for bladder cancer (BCa) patients in different m6 A-associated lncRNA-derived risk groups. **F** The correlation between m6 A-associated lncRNA-derived risk scores and tumor mutational burden (TMB). **G** The survival analysis of bladder cancer (BCa) patients grouped by the combination of tumor mutational burden (TMB) levels and the m6 A-associated lncRNA-derived risk groups

A significant challenge in treating BCa cells is their ability to evade immune system attacks through various mechanisms, undermining the effectiveness of immunotherapy [21]. Tumor-associated macrophages (TAMs) are key contributors to lymph node (LN) metastasis in the tumor microenvironment, particularly in BCa. Interestingly, lncRNA LNMAT1 was linked to the promotion of lymphangiogenesis by epigenetically activating CCL2 expression. Moreover, lncRNA LNMAT1 recruits hnRNPL to the CCL2 promoter, enhancing transcription by triggering H3 K4 tri-methylation. The high CCL2 levels attract macrophages to the tumor site, which promote lymphatic metastasis via VEGF-C secretion [22]. A study revealed that FGF9 and the lncRNA LINC01140 are upregulated in BCa, enhancing M2 polarization, and the knockdown promotes M1 macrophage polarization. LINC01140, miR-140-5p, and FGF9 form a regulatory axis, where LINC01140 modulates FGF9 through miR-140-5p, influencing BCa progression and macrophage polarization [23]. As regards the role of lncRNAs in BCa intratumor fibroblast formation, lncRNA CYTOR is an oncogene that promotes M2 macrophage polarization and interacts with cancer-associated fibroblasts (CAFs). Furthermore, the expression of CYTOR correlates with PD-1/PD-L1 expression, indicating its potential as a biomarker for predicting survival outcomes [24]. Further, CAF-conditioned medium enhanced BCa cell invasion by inducing epithelial-mesenchymal transition (EMT) through high transforming growth factor-β–1 (TGFβ1) levels, which phosphorylates Smad2 and regulates EMT-associated markers [25]. Another study showed that ncRNA LINC00665 promoted CAF infiltration, which is linked to LN metastasis and poor prognosis in BCa patients. LINC00665 enhances RAB27B expression and subsequent EV secretion, leading to a CAF phenotype and forming a RAB27B-HGF-c-Myc positive feedback loop that drives BCa lymphangiogenesis [26].

We identified TP53 as the most differentially mutated gene among BCa patients within different m6 A-associated lncRNA-derived risk groups. Additionally, lncRNA XIST has been identified as a significant regulator of cell cycle and migration in BCa cells. XIST exerts its effects by binding with TET1, which subsequently downregulates the tumor suppressor p53, highlighting a crucial function of the XIST-TET1-p53 regulatory network in BCa pathogenesis [27]. LncRNA H19 enhances cancer cell proliferation by inhibiting p53 activation and altering the expression of Bax/Bcl-2 and cyclin D1, which disrupts normal cell cycle regulation [28]. Further, lncRNA LOC572558 promotes apoptosis in BCa cells through the dephosphorylation of AKT and MDM2 and the phosphorylation of p53, suggesting that LOC572558 regulates the

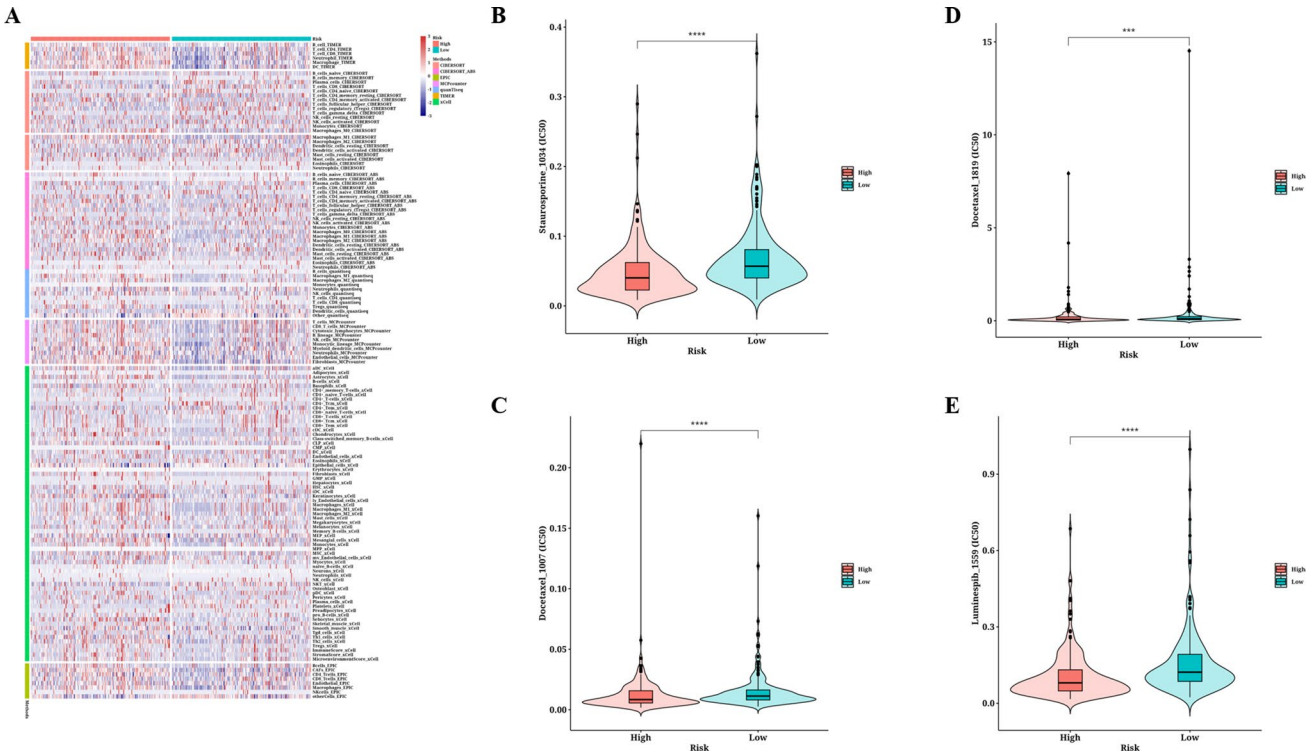

Fig. 8 Immune cell infiltration and drug sensitivity analysis of N6-methyladenosine (m6 A)-associated lncRNA-derived Risk Groups. **A** The heatmap displaying the extent of immune and immune regulatory cell infiltration in each bladder cancer (BCa) sample using a variety of bioinformatics-based approaches. **B**–**E** Drug sensitivity analysis assessing the half-maximal inhibitory concentration (IC50) value of Staurosporine_1034 (**B**) and Docetaxel_1007 (**C**), Docetaxel_1819 (**D**), and Luminespib_1559 (**E**) in bladder cancer (BCa) patients with different m6 A-associated lncRNA-derived risk scores

p53 signaling pathway [29]. These findings highlight the potential of lncRNAs as therapeutic targets by regulating TP53 for treating BCa.

5 Conclusion

Our findings highlight the prognostic value and clinical relevance of m6 A-associated lncRNAs in BCa, offering new insights into patient stratification and personalized therapy approaches.

Acknowledgements Not applicable.

Author contribution Renhu Chen: conceptualization, data curation, Yuqing Ye methodology, Yuxuan Zheng: data curation. project administration.project administration, supervision.Ethics approval and consent to participateNot applicable.

Funding Not applicable.

Availability of data and materials The datasets generated during and/or analysed during the current study are available from the corresponding author on reasonable request.

Declarations

Ethics approval and consent to participate Not applicable.

Consent for publication Not applicable.

Competing interests The authors declare no competing interests.

Open Access This article is licensed under a Creative Commons Attribution-NonCommercial-NoDerivatives 4.0 International License, which permits any non-commercial use, sharing, distribution and reproduction in any medium or format, as long as you give appropriate credit to the original author(s) and the source, provide a link to the Creative Commons licence, and indicate if you modified the licensed material. You do not have permission under this licence to share adapted material derived from this article or parts of it. The images or other third party material in this article are included in the article's Creative Commons licence, unless indicated otherwise in a credit line to the material. If material is not included in the article's Creative Commons licence and your intended use is not permitted by statutory regulation or exceeds the permitted use, you will need to obtain permission directly from the copyright holder. To view a copy of this licence, visit http://creativecommons.org/licenses/by-nc-nd/4.0/.

References

1. Siegel RL, Miller KD, Wagle NS, Jemal A. Cancer statistics. CA Cancer J Clin. 2023;73(1):17–48.
2. Siegel RL, Miller KD, Jemal A. Cancer statistics. CA Cancer J Clin. 2018;68(1):7–30.
3. Viveiros N, Flores BC, Lobo J, et al. Detailed bladder cancer immunoprofiling reveals new clues for immunotherapeutic strategies. Clin Transl Immunology. 2022;11(9): e1402.
4. Knowles MA, Hurst CD. Molecular biology of bladder cancer: new insights into pathogenesis and clinical diversity. Nat Rev Cancer. 2015;15(1):25–41.
5. Akhavan-Niaki H, Samadani AA. DNA methylation and cancer development: molecular mechanism. Cell Biochem Biophys. 2013;67(2):501–13.
6. Roignant JY, Soller M. m(6)A in mRNA: an ancient mechanism for fine-tuning gene expression. Trends Genet. 2017;33(6):380–90.
7. Hirota T, Tanaka T, Takesue H, Ieiri I. Epigenetic regulation of drug transporter expression in human tissues. Expert Opin Drug Metab Toxicol. 2017;13(1):19–30.
8. Zhang Y, Chen X, Lin J, Jin X. Biological functions and clinical significance of long noncoding RNAs in bladder cancer. Cell Death Discov. 2021;7(1):278.
9. Wei CM, Gershowitz A, Moss B. Methylated nucleotides block 5′terminus of HeLa cell messenger RNA. Cell. 1975;4(4):379–86.
10. Jianfeng W, Yutao W, Jianbin B. Long non-coding RNAs correlate with genomic stability in prostate cancer: a clinical outcome and survival analysis. Genomics. 2021;113(5):3141–51.
11. Wang Y, Yan K, Wang L, Bi J. Genome instability-related long non-coding RNA in clear renal cell carcinoma determined using computational biology. BMC Cancer. 2021;21(1):727.
12. Zhang L, Li Y, Zhou L, et al. The m6A reader YTHDF2 promotes bladder cancer progression by suppressing RIG-I-mediated immune response. Cancer Res. 2023;83(11):1834–50.
13. Dhamija S, Diederichs S. From junk to master regulators of invasion: lncRNA functions in migration. EMT Metastasis Int J Cancer. 2016;139(2):269–80.
14. Pilala KM, Panoutsopoulou K, Papadimitriou MA, Soureas K, Scorilas A, Avgeris M. Exploring the methyl-verse: dynamic interplay of epigenome and m6A epitranscriptome. Mol Ther. 2025;33(2):447–64.
15. Hu J, Wang L, Li L, Wang Y, Bi J. A novel focal adhesion-related risk model predicts prognosis of bladder cancer—a bioinformatic study based on TCGA and GEO database. BMC Cancer. 2022;22(1):1158.
16. Sun S, Wang Y, Wang J, Bi J. Wnt pathway-related three-mRNA clinical outcome signature in bladder urothelial carcinoma: computational biology and experimental analyses. J Transl Med. 2021;19(1):409.
17. Su H, Wang Y, Li H. RNA m6A methylation regulators multi-omics analysis in prostate cancer. Front Genet. 2021;12: 768041.
18. Zheng R, Gao F, Mao Z, et al. LncRNA BCCE4 genetically enhances the PD-L1/PD-1 interaction in smoking-related bladder cancer by modulating miR-328-3p-USP18 signaling. Adv Sci (Weinh). 2023;10(30): e2303473.
19. Liu Y, Liu Y, Ye S, Feng H, Ma L. A new ferroptosis-related signature model including messenger RNAs and long non-coding RNAs predicts the prognosis of gastric cancer patients. J Transl Int Med. 2023;11(2):145–55.
20. Luo W, Wang J, Xu W, et al. LncRNA RP11-89 facilitates tumorigenesis and ferroptosis resistance through PROM2-activated iron export by sponging miR-129-5p in bladder cancer. Cell Death Dis. 2021;12(11):1043.
21. Xie J, Zhang H, Wang K, et al. M6A-mediated-upregulation of lncRNA BLACAT3 promotes bladder cancer angiogenesis and hematogenous metastasis through YBX3 nuclear shuttling and enhancing NCF2 transcription. Oncogene. 2023;42(40):2956–70.
22. Chen C, Zheng H, Luo Y, et al. SUMOylation promotes extracellular vesicle-mediated transmission of lncRNA ELNAT1 and lymph node metastasis in bladder cancer. J Clin Invest. 2021;131(8): e146431.
23. Yang Z, Xu Y, Bi Y, et al. Immune escape mechanisms and immunotherapy of urothelial bladder cancer. J Clin Transl Res. 2021;7(4):485–500.
24. Chen C, He W, Huang J, et al. LNMAT1 promotes lymphatic metastasis of bladder cancer via CCL2 dependent macrophage recruitment. Nat Commun. 2018;9(1):3826.
25. Wu S, Xu R, Zhu X, et al. The long noncoding RNA LINC01140/miR-140-5p/FGF9 axis modulates bladder cancer cell aggressiveness and macrophage M2 polarization. Aging (Albany NY). 2020;12(24):25845–64.
26. Wu Y, Xu Y, He S, et al. Cytoskeleton regulator RNA expression on cancer-associated fibroblasts is associated with prognosis and immunotherapy response in bladder cancer. Heliyon. 2023;9(3): e13707.
27. Zhuang J, Lu Q, Shen B, et al. TGFβ1 secreted by cancer-associated fibroblasts induces epithelial-mesenchymal transition of bladder cancer cells through lncRNA-ZEB2NAT. Sci Rep. 2015;5:11924.
28. Li Y, Zheng H, Luo Y, et al. An HGF-dependent positive feedback loop between bladder cancer cells and fibroblasts mediates lymphangiogenesis and lymphatic metastasis. Cancer Commun (Lond). 2023;43(12):1289–311.
29. Hu B, Shi G, Li Q, Li W, Zhou H. Long noncoding RNA XIST participates in bladder cancer by downregulating p53 via binding to TET1. J Cell Biochem. 2019;120(4):6330–8.

Publisher's Note Springer Nature remains neutral with regard to jurisdictional claims in published maps and institutional affiliations.